Design and Analysis of a Bionic Skate Based on MPF Movement Patterns

Tielin Yan, Xiaochun Li, Zengrui Li, Yiran Feng*

Dalian Polytechnic University Dalian, China

* Corresponding Author Email: fengyr@dlpu.edu.cn

Abstract. This paper uses pectoral fins fluctuation pattern class triangular skate as the object of study. The skate generates waveforms through its broad pectoral fins, which are transmitted backwards to push the water backwards, and the reaction force of the water obtained is the forward thrust i.e. the MPF pattern. The fins are designed to meet the fluctuation pattern of the sinusoidal function. A prototype pectoral fin of the ray is analysed to establish the kinematic model of the fluttering wing, the envelope coefficients are designed to decouple and simplify the kinematic equations, and a three-dimensional mesh is drawn using MATLAB; fluid simulation is carried out by Fluent to obtain the vortex cloud; the bionic ray is tested and tested to meet the actual requirements.

Keywords: bionic skate, MPF motion pattern, Fluent, vortex cloud.

1. Introduction

The application of the fishtail imitation thruster will change the current situation where the propeller thruster and rudder system are separate and complex, and achieve a combined paddle-rudder function[1]. The fin fluctuations will drive the water backwards in a more energy-efficient manner, while generating vortices in the same direction as the propulsion, giving it more desirable hydrodynamic properties and thus improving efficiency.

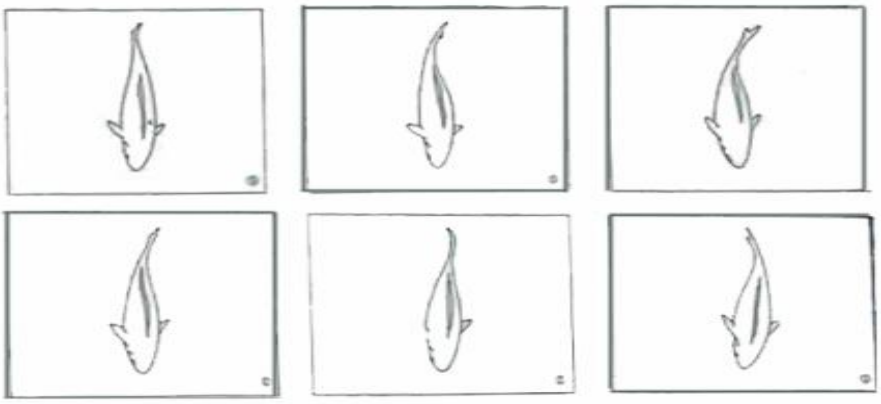


Figure 1. BCF swimming diagram

The significant difference between the MPF and BCF modes “Fig.1”is that the BCF mode produces forward propulsion mainly through the body and the flapping of the caudal fins, while the MPF mode has significant advantages over the BCF mode in terms of propulsion efficiency, manoeuvrability and noise due to the flexible propulsion system of the pectoral fins, which are composed of multi-jointed cartilage and muscle groups.[2]The MPF mode of propulsion has significant advantages over the BCF mode in terms of propulsion efficiency, manoeuvrability and noise.

There are currently three main types of MPF propulsion mode fish designs in the world:

(1) The static 2D pectoral fin of Manta Droid, National University of Singapore. The design is a significant simplification of the pectoral fin model, with the overall solidification of the pectoral fin being unable to be deformed. Only the up and down undulating oscillation of the 2D spreading plane is retained.

(2) Dynamic 3D pectoral fins from Aqua Ray, Festo, Germany. The individual fin units cannot be controlled independently and the pectoral fin wing shape cannot be maintained in the water.

(3) Pneumatic soft-bodied manta rays from Osaka University, Japan. The fin surface and the body are made of silicone rubber, again it is not possible to subdivide the pectoral fin motor unit and remains a single degree of freedom pectoral fin.

This paper designs a three-dimensional fin-like thruster with a three-dimensional airfoil pattern, consisting of 5-8 crank-linked kinematic units, to achieve controlled airfoil deformation with multiple degrees of freedom. The bionic underwater vehicle with MPF motion mode has excellent manoeuvrability and stability at low speeds and can hover in real time.

The structure of this design is roughly divided into 5 parts “Fig.2”: the bionic fish head, the bionic spine, the soft pectoral fin, the drive linkage and the balanced fish tail.

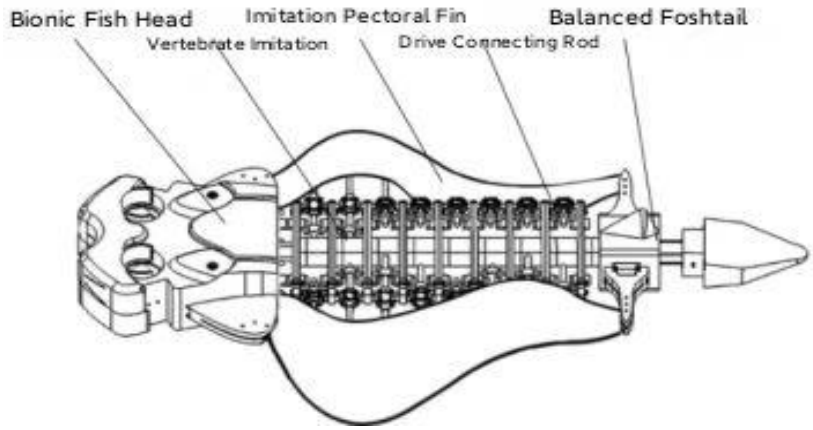


Figure 2. Bionic skate structural design

The head is the control and power unit and is equipped with a pair of fans to provide auxiliary thrust to the skate for ascent and dive.

The fins on both pectoral fins oscillate periodically and symmetrically from front to back as the fish swims steadily. Because of the phase delay between the fins and the sinusoidal oscillation of the fins, the fin surface forms a sinusoidal propulsion wave from front to back.

While the pectoral fins push the fluid backwards, the fluid in turn acts on the pectoral fins to give the machinefish thrust and forward movement. “Fig.3” The forward speed of the machinefish is directly related to the fluid forces, which are mainly determined by the shape of the fin surface of the pectoral fins and the oscillation speed of the fins.

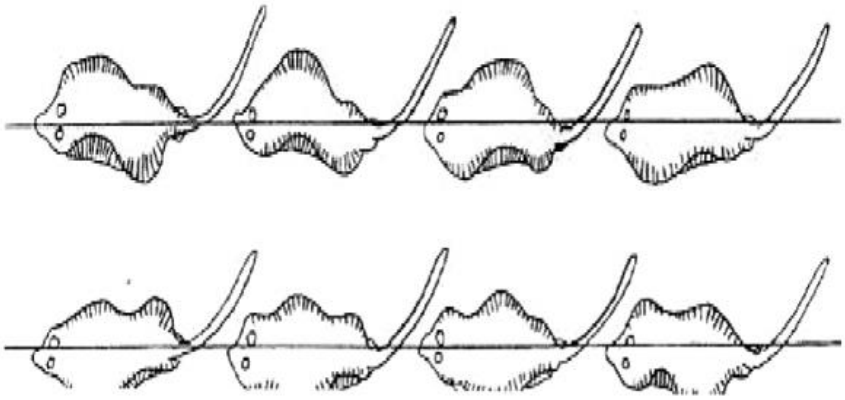


Figure 3. Sketch of MPF movement

The oscillation speed of the fins is proportional to the fin swing and the fin swing frequency, while the shape of the pectoral fin surface is mainly related to the phase difference of the adjacent fins. By varying the motion parameters such as the amplitude of the fins, the frequency of the fins and the phase difference of the adjacent fins respectively, a series of movements of the robot fish can be achieved. At the same time a rudder is mounted on the tail, which, in combination with the BCF motion mode, controls the oscillation of the fish's tail, acts as a rudder, controls the left and right movements of the robot fish and increases the auxiliary thrust.

Following the propulsion of the ray MPF, the head of the bionic ray is equipped with a motor to drive the oscillation of the fins. The movement of the fins deforms the multi-degree-of-freedom controlled fin surface , and the crank slider on the fins , by the rotation of the motor transforms the rotation into an up-and-down reciprocating oscillation . “Fig.4”

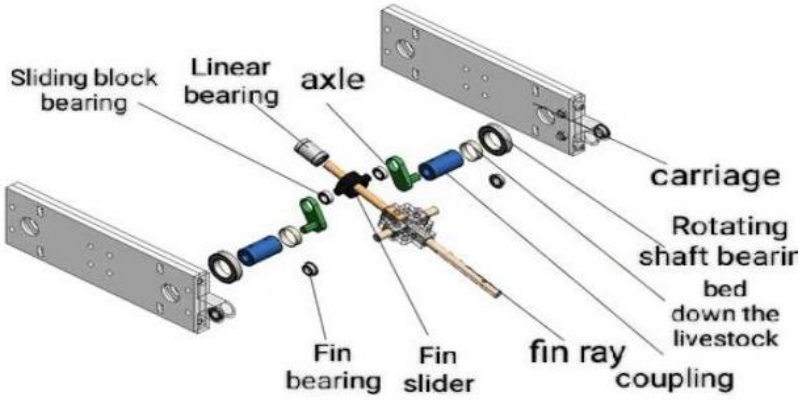


Figure 4. Schematic diagram of the drive linkage structure

2. Bionic kinematic modelling

2.1. Five fin strip flutter design

Pectoral fins of the physical characteristics and motion parameters determine the pectoral fin motion when the hydrodynamic component and can affect the fish propulsion and maneuvering physical characteristics including article fin spacing, fin length and fins of flexible; The motion parameters mainly include the amplitude, the wave frequency, the wave wavelength and the phase between the fins. Next we will model pectoral fin motion based on these data.

Blevins et al. experimentally measured the variation in the amplitude of pectoral fin fluctuations along the span and chord lengths of the skate as it cruised, marking points on the upper surface of the skate in both directions, and quantifying the increase in pectoral fin fluctuations along both the span and chord lengths “Fig.5”. Each fin is driven by the muscles on either side of it, which alternately contract and elongate to achieve a reciprocal flexible movement of the fin[3] .

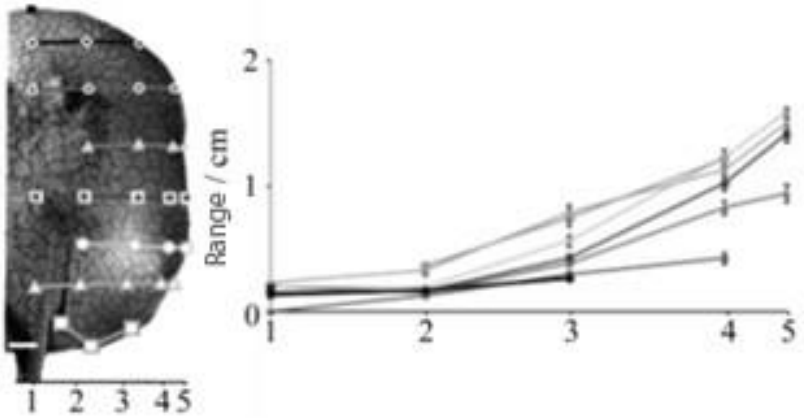


Figure 5. Variation in the amplitude of pectoral fin fluctuations along the span and chord length of the skate

In this paper, a flat-bodied cartilaginous fish, the skate, is used as a reference object for the design of a five-fin flutter wing. The bionic pectoral fin test model motion is driven by five fins, and the sinusoidal periodic motion pattern of the fins is as follows:

$$\theta_{11}(t) = A\sin(2\pi ft) \quad (1)$$

$$\theta_{12}(t) = A\sin(2\pi ft - \Delta\varphi) \quad (2)$$

$$\theta_{13}(t) = A\sin(2\pi ft - 2\Delta\varphi) \quad (3)$$

$$\theta_{14}(t) = A\sin(2\pi ft - 3\Delta\varphi) \quad (4)$$

$$\theta_{15}(t) = A\sin(2\pi ft - 4\Delta\varphi) \quad (5)$$

where θ_{11} , θ_{12} , θ_{13} , θ_{14} , θ_{15} are the angles of the left front, middle and rear fins to the plumb plane, respectively; A is the angular amplitude, f is the oscillation frequency in Hz and $\Delta\varphi$ is the fin phase difference.

The larger the phase difference is, the thrust of the flexible pectoral fin first increases and then decreases, and the maximum value of the periodic oscillation of each force and torque coefficient also decreases. It can be inferred that there is an optimal phase difference that maximizes the thrust of the flexible pectoral fin.

2.2. Equation of Motion Design

As the frequency increases, the positive thrust on the flexible pectoral fins. The mean value is decreasing, which means that the net thrust is increasing at this point, i.e. the mean value of thrust increases approximately linearly with increasing frequency. In addition, the maximum magnitude of the periodic oscillations of the forces and moment coefficients increases approximately linearly with increasing frequency. If the kinematic equation for the pectoral fin is centred on describing the state of motion of the fin surface “Fig.6”, it can be expressed as:

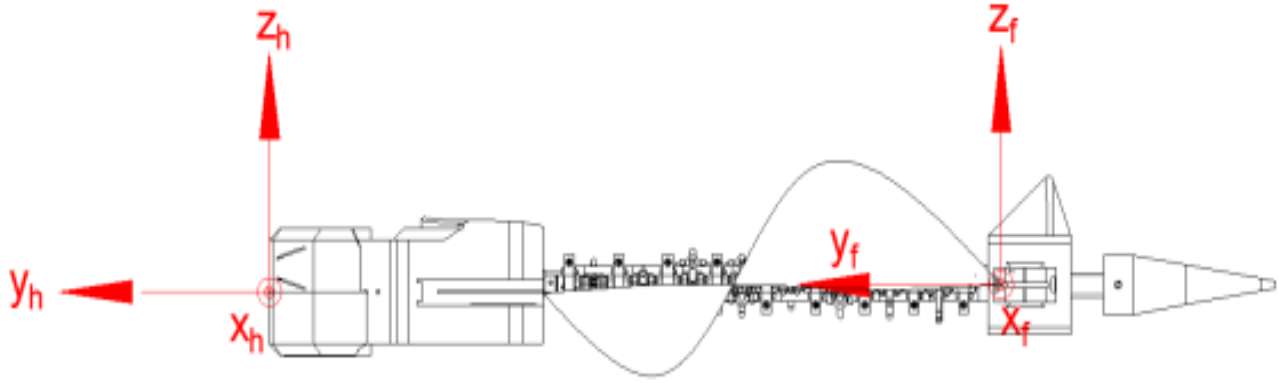


Figure 6. Definition of pectoral fin co-ordination

$$z(t) = h(x, y, t), (x, y) \in S, x > 0, y > 0 \quad (6)$$

where S is the projected area of the pectoral fin in the XY plane.

The chordal fluctuations of the propulsive wave on the pectoral fin are similar to a sine wave, and the extensive deformation in the spreading direction is approximated as a quadratic curve, then the propulsive wave envelope is a curved surface Since the pectoral fin surface wave is a composite of the motion in the chordal and spreading directions, it is assumed that any chordal position of the pectoral fin has the same proportion of spreading deformation, and the pectoral fin spreading wave amplitude envelope behaves as a quadratic curve.*h* is the displacement of the point on the pectoral fin in the direction of z ;c_1, c_2 is the envelope coefficient, the value of which is related to the pectoral fin flapping pattern and other factors;*f* is the pectoral fin oscillation frequency;$k = \frac{2\pi}{\lambda}$ is the wave number of the pectoral fin propulsion wave and λ is the wavelength.

The curve (Fig. 7) wave amplitude function can be decoupled for x,y. The equation of pectoral fin motion can then be simplified to[4]:

$$z(t) = h(x, y, t) = (c_1 y_1 + c_2 y_2)\sin(2\pi ft - kx) \quad (7)$$

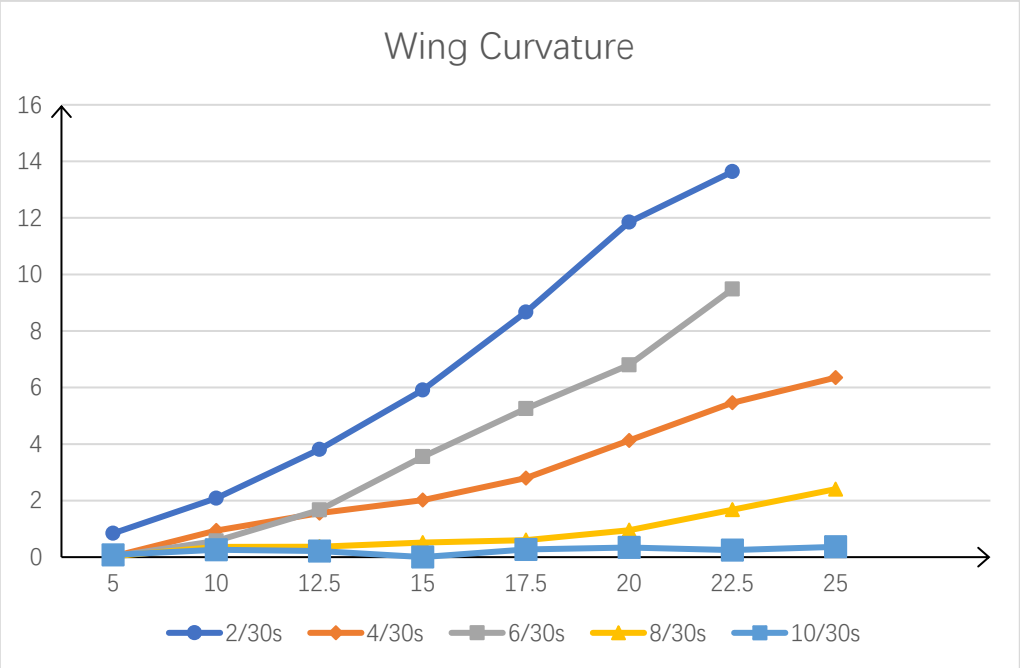


Figure 7. Time course of pectoral fin spread displacement (1/4 cycle)

where $c_1$and c_2 are envelope coefficients whose values are dependent on factors such as the way the pectoral fins are flapped. The spreading wave amplitude distribution can be controlled by controlling the magnitude of the parameters c_1 and c_2. The fmesh function is used in MATLAB to plot the 3D mesh. “Fig.8-Fig.9”

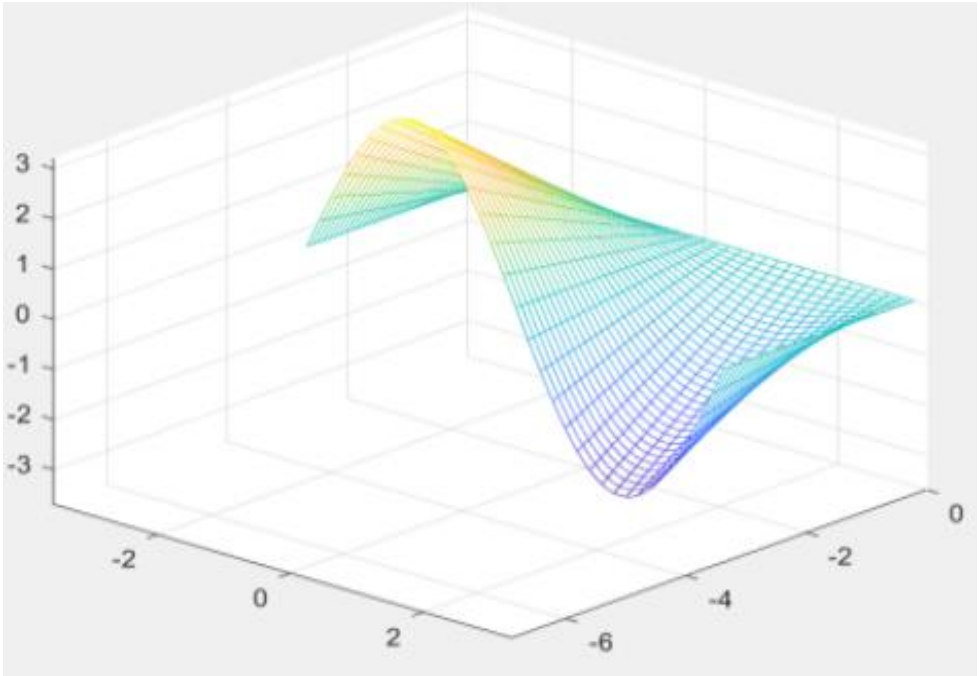


Figure 8. Motion waveform

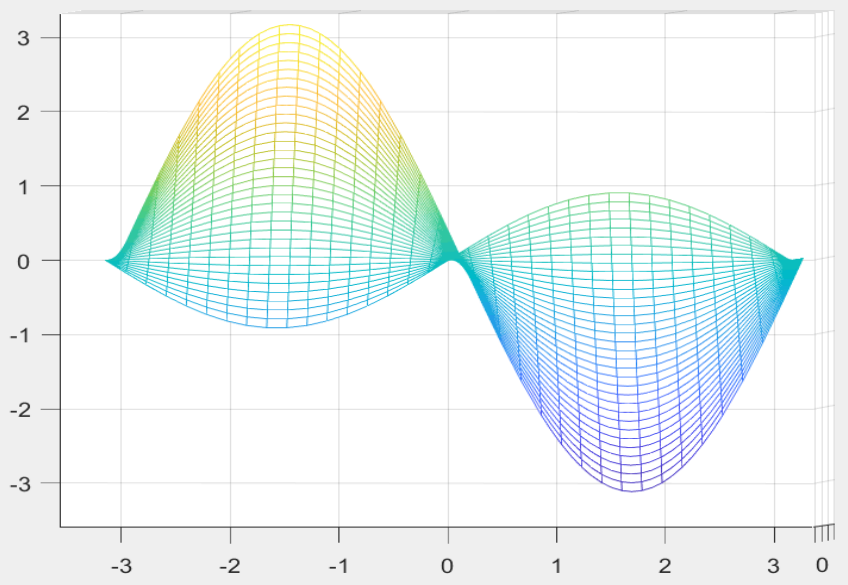


Figure 9. Chordwise waveform

3. Simulated Analysis

3.1. Fin Surface Material

The body of the flexible pectoral fins uses a two-component platinum-catalyzed silicone rubber as a superelastic, large deformable, approximately incompressible, non-linear material is based on the second order Yeoh model to establish the material proprieties of a soft pectoral fin, whose energy density function can be expressed as

$$W = C_{10}\left(\lambda^2 + \frac{1}{\lambda^2} - 2\right) + C_{20}\left(\lambda^2 + \frac{1}{\lambda^2} - 2\right)^2 \tag{8}$$

where λ is the main elongation ratio and polynomial coefficients c_{10}, c_{20} by Abaqus Material Evaluation tool calculates[5]; c_{10}=0.11, c_{20}=0.02; material fit data based on ASTM D412 standard tensile test[6].

3.2. Fluid Simulation

The above model does not take into account the fluid environment and only reflects the pectoral fin movement. In fact, when fish swim in water, they move and deform under the action of hydrodynamic force. At the same time, the deformation of fish body changes the boundary conditions of fluid surface, which changes the hydrodynamic force.

Applying Newton's second law $\sum F = ma$ to the micro-elementary hexahedron, a differential equation of motion expressed in terms of stresses can be derived. Due to the small effect of the thickness of the pectoral fin material on the motion, only the effect of stresses in the upper and lower planes is considered. The final derivation is as follows:

$$\tau_{xy} = \tau_{yx} = \mu\left(\frac{\partial v_x}{\partial y} + \frac{\partial v_y}{\partial x}\right), \quad P_{xx} = P - 2\mu\frac{\partial v_x}{\partial x} \tag{9}$$

$$\tau_{yz} = \tau_{zy} = \mu\left(\frac{\partial v_y}{\partial z} + \frac{\partial v_z}{\partial y}\right), \quad P_{yy} = P - 2\mu\frac{\partial v_y}{\partial y} \tag{10}$$

$$\tau_{zx} = \tau_{xz} = \mu\left(\frac{\partial v_z}{\partial x} + \frac{\partial v_x}{\partial z}\right), \quad P_{zz} = P - 2\mu\frac{\partial v_z}{\partial z} \tag{11}$$

Imitating Newton's law of internal friction, the relationship between stress and deformation for three-dimensional shear flow gives:

$$f_z - \frac{1}{\rho}\left(-\frac{\partial \tau_{xz}}{\partial x} - \frac{\partial \tau_{yz}}{\partial y} + \frac{\partial P_{zz}}{\partial z}\right) = \frac{dv_z}{dt} \tag{12}$$

According to the above formula, when the fluid flows through the pipe, the higher the fluid velocity, the greater the friction force and the greater the fluid friction loss. This is because the friction force is determined by the contact area and speed between the fluid and the inner wall of the pipe. The greater the flow rate, the greater the contact area, and therefore the greater the friction force.

Fluent a computational fluid dynamics software, was applied to analyse the effect of flutter pattern and surrounding airflow environment on the aerodynamic performance of the bionic flutter aircraft. "Fig.11" Set the pectoral fin flutter speed and angular velocity[7].

Table 1. simulation parameter

Data Type		Numerical Value
Reynolds factor	R_e	1.01 × 103
Pitch range of motion	θ_m	10°, 20°, 30°
Pitch pivot position	X_p	c/4, c/3,c/2,2c/3
Phase difference/(°)	ψ	0-51°
Fluid field size/(mm)		200mm x 200mm
Flap size/(mm)		0.3mm x 0.005mm
Simulation time/(s)	s	4~15s
Fluid density/(kg/m3)		10^3kg/m^3

The three-dimensional space is divided into countless tiny voxels to form a grid. Design initial values and boundary conditions on a grid. The simulation parameters were set in ANSYS Fluent according to the parameters in the above table, including the selection of initial conditions and the upper and lower limits of physical parameters.

In the simulation process, the fin pressure diagram can be presented in real time, as shown in Figure 10.

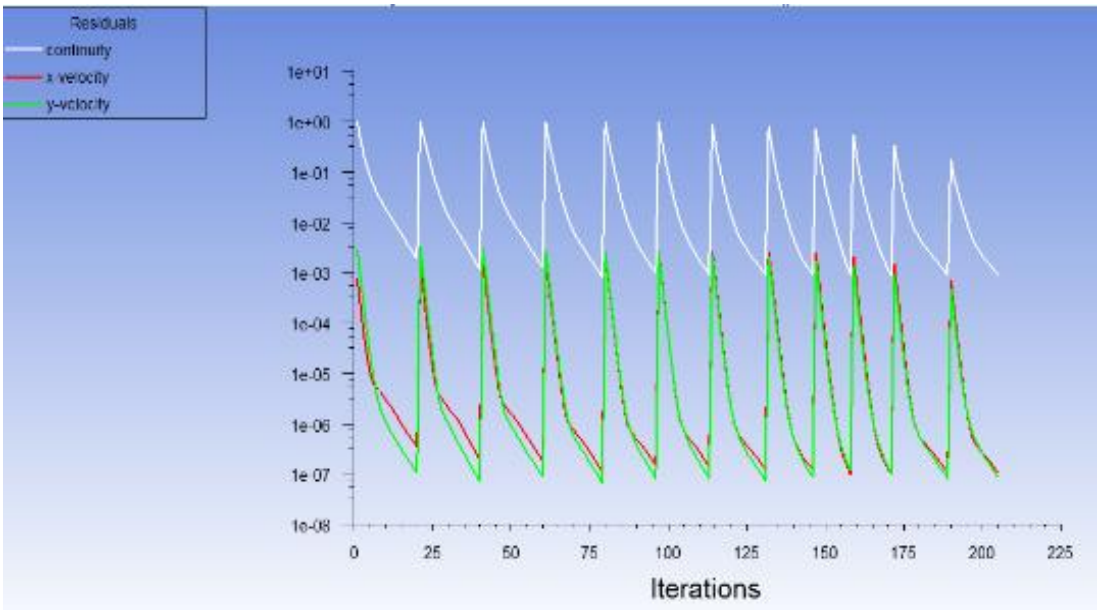


Figure 10. Real-time pressure map of flutter motion

The simulation data were derived and processed through Tecplot to obtain the two-dimensional vorticity nephogram of pectoral fin movement as shown in Figure 11. According to the vorticity cloud map, there is a pressure difference between the upper and lower pectoral fins during the movement, which can promote the bionic ray to move.

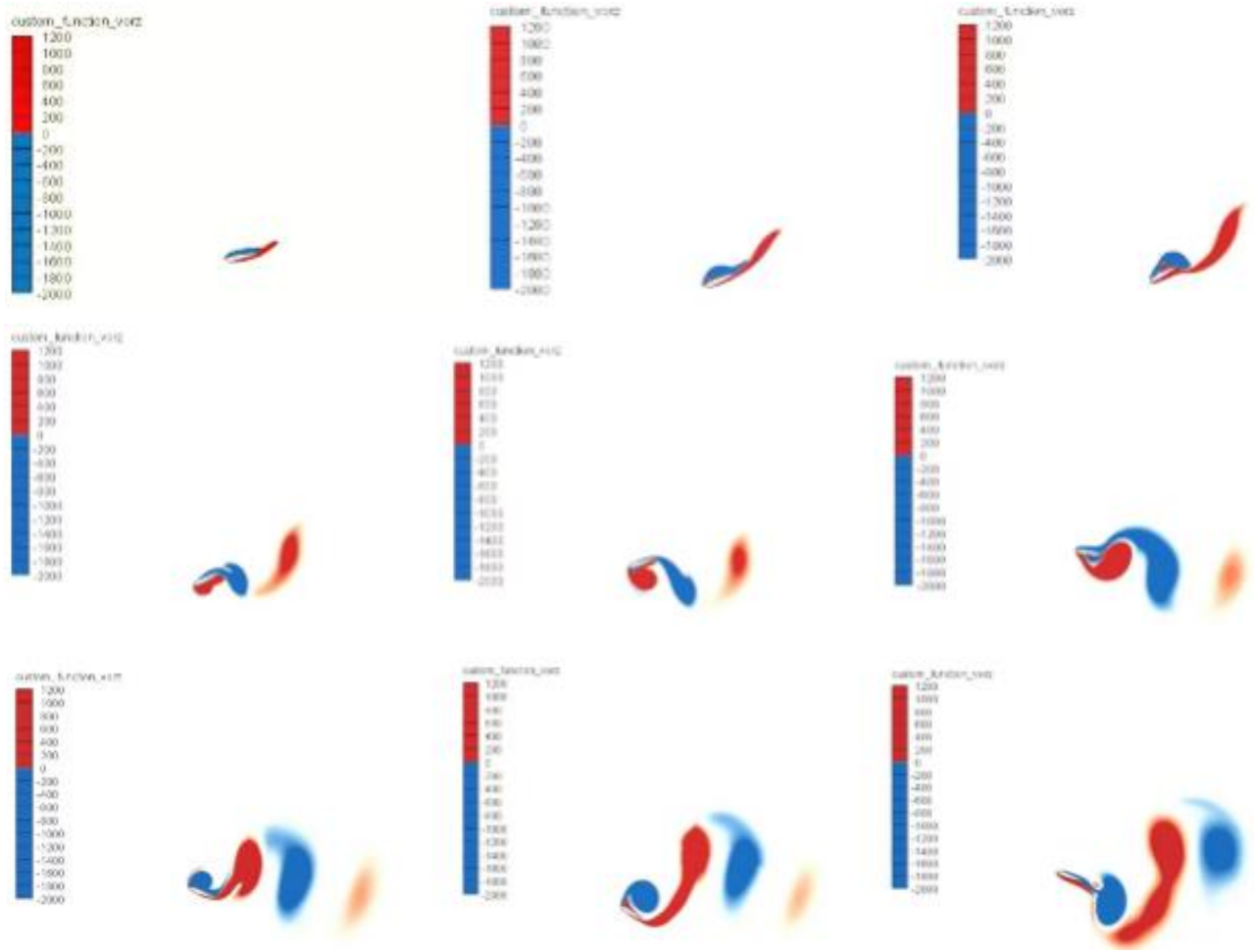


Figure 11. Pectoral fin vortex volume cloud

Video of the skate cruising in a straight line and analysed frame by frame to obtain a sequence of axial pectoral fin movements during a complete flutter cycle. “Fig.12”

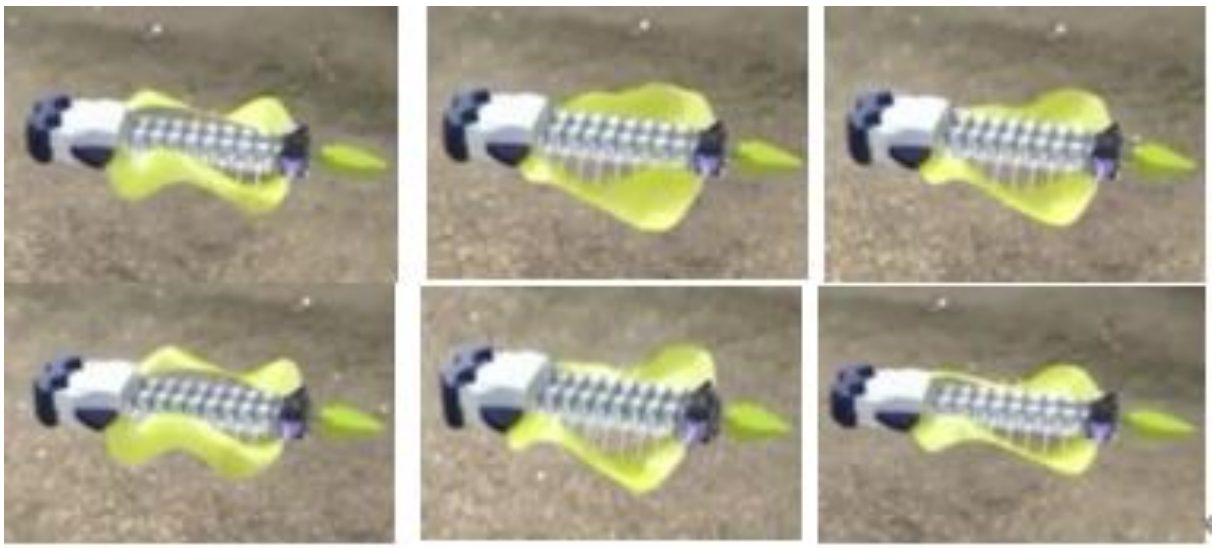


Figure 12. Fin flap timing diagram - axial view

4. Conclusion

(1) A five-fin pectoral fin with equal phase difference is designed after a ray. The movement of the pectoral fin can form a sinusoidal propulsion wave, which can provide sufficient power for the movement of the bionic ray.

(2) As frequency increases, the mean value of the forward thrust on the flexible pectoral fin decreases, indicating that the net thrust is increasing at this point, i.e. the mean thrust increases approximately linearly with increasing frequency.

(3) The kinematic model of the pectoral fin mode of the skate was decoupled and simplified by designing modified kinematic parameters for the pectoral fin mode of the skate.

(4) The idea of finite elements was applied and Fluent simulation was used to discretize the continuous space into a certain number of control bodies, thus allowing the system of partial differential equations in fluid dynamics to be solved and a two-dimensional pectoral fin vorticity cloud was derived.

(5) The bionic skate has been experimentally tested to meet practical needs.

Acknowledgments

Corresponding author, Feng Yiran, fengyr@dlpu.edu.cn, School of Mechanical Engineering and Automation, DalianPolytechnic University Liaoning, China.

This work was financially supported by: Dalian Young Stars of Science and Technology Project (NO.2021RQ088), Higher Education Research Project of Dalian Polytechnic University in 2022 and Innovation and Entrepreneurship Incubation Base Pro-ject of Dalian Polytechnic University, 2023 Dalian Polytechnic University Education and Teaching Reform Project.

References

[1] L. Chen, S. Bi, Y. Cai, Y. Cao, and G. Pan, “Design and Experimental Research on a Bionic Robot Fish with Tri-Dimensional Soft Pectoral Fins Inspired by Cownose Ray,” *JMSE*, vol. 10, no. 4, pp. 537, Apr. 2022.

[2] J. Kadiyam and S. Mohan, “Conceptual design of a hybrid propulsion underwater robotic vehicle with different propulsion systems for ocean observations,”*J. Waterw. Port Coastal Ocean Eng.*, vol. 182, pp. 112–125, Jun. 2019.

[3] C.D. Wilga and G. V. Lauder, “Function of the heterocercal tail in sharks: quantitative wake dynamics during steady horizontal swimming and vertical maneuvering,” *J. Exp. Biol.*, vol. 205, no. 16, pp. 2365–2374, Aug. 2002.

[4] K. D. von Ellenrieder, K. Parker, and J. Soria, “Fluid mechanics of flapping wings,” *Exp. Therm Fluid Sci*., vol. 32, no. 8, pp. 1578–1589, Sep. 2008.

[5] S. LI, H. JIA, M. LI, et al., “Theory and special experiment methods of the constitutive model of hyper-elastic material.” *China Elastomerics*, vol. 21, no. 1, pp. 58-64, 2011.

[6] N. Elango, N. S. Gupta, Y. Lih Jiun, and A. Golshahr, “The Effect of High Loaded Multiwall Carbon Nanotubes in Natural Rubber and Their Nonlinear Material Constants,” *J. Nanomater*, vol. 2017, pp. 1–15, 2017.

[7] A.Zhang, P.Sun., F.Ming., and A.Colagrossi , “Smoothed particle hydrodynamics and its applications in fluid-structure interactions,” *J. Hydrodyn. Ser. B*, vol. 29, no. 2, pp. 187–216, 2017.

[8] R.W. Blake, “Fish functional design and swimming performance,” J. Fish Biol., vol. 65, no. 5, pp. 1193–1222, Nov. 2004.

[9] M.S. Triantafyllou, F. S. Hover, A. H. Techet, and D. K. P. Yue, “Review of Hydrodynamic Scaling Laws in Aquatic Locomotion and Fishlike Swimming,”Appl. Mech. Rev., vol. 58, no. 4, pp. 226–237, Jul. 2005.

[10] Z. Wang et al., “Review of multi-fin propulsion and functional materials of underwater bionic robotic fish,” Proceedings of the Institution of Mechanical Engineers, Part C: J. Mech. Eng. Sci., vol. 236, no. 13, pp. 7350–7367, Jul. 2022.

[11] Y. ISODA, Y. TANAKA, M. KAWANO, and S. MURATA, "Effect of Phase Difference Between Pitching Foil and Periodic Flow on Maneuverability in the Lift Direction." JSEM, vol. 7, Iss. 0, pp.34-42, Aug. 2022.

[12] Z. Qi, L. Jia, Y. Qin, J. Shi, and J. Zhai, "Propulsion Performance of the Full-Active Flapping Foil in Time-Varying Freestream," Appl. Sci., vol. 10, no. 18, pp. 6226, Sep. 2020.